

LARGE SCALE QSO-GALAXY CORRELATIONS AND WEAK LENSING

Liliya L.R. Williams

Department of Physics and Astronomy

University of Victoria

Victoria, BC, V8P 1A1, Canada

ABSTRACT

Several recent studies show that bright, intermediate and high redshift optically and radio selected QSOs are positively correlated with nearby galaxies on a range of angular scales up to a degree. Obscuration by unevenly distributed Galactic dust can be ruled out as the cause, leaving weak statistical lensing as the physical process responsible. However the amplitude of correlations on $\lesssim 1^\circ$ angular scales is at least a factor of a few larger than lensing model predictions. A possible way to reconcile the observations and theory is to revise the weak lensing formalism. We extend the standard lensing formulation to include the next higher order term (second order) in the geodesic equation of motion for photons. We derive relevant equations applicable in the weak lensing regime, and discuss qualitative properties of the updated formulation. We then perform numerical integrations of the revised equation and study the effect of the extra term using two different types of cosmic mass density fluctuations. We find that *nearby large-scale coherent* structures increase the amplitude of the predicted lensing-induced correlations between QSOs and foreground galaxies by $\sim 10\%$ (not a factor of several required by observations), while the redshift of the optimal, i.e. ‘most correlated’ structures is moved closer to the observer compared to what is predicted using the standard lensing equation.

1. Introduction

Weak gravitational lensing manifests itself in two observable ways: if a source is extended, like a galaxy, its image will appear to be sheared tangentially with respect to the foreground mass concentration. If sources are unresolved, like QSOs, weak lensing can be detected in a statistical way by the sources’ angular (anti)correlation with the tracers of the intervening mass distribution.

Statistical QSO-galaxy associations on large angular scales, $10' - 1^\circ$ are the subject of the present paper. The mechanism responsible for the associations is believed to be the magnification bias, which depends on the shape of the number-magnitude counts of the background sources. If the number counts are a power law with a slope $\alpha = d\log N(m)/dm$ then the over- or underdensity of sources down to a certain limiting flux behind the lens is related to the lens magnification M by $q(M, \alpha) = M^{2.5\alpha-1}$. The factor 2.5α in the exponent accounts for the magnification of individual

sources brightened into a flux limited sample, while the factor M^{-1} corrects for the area dilution of the number density of sources on the sky. Thus if $\alpha > 0.4$ ($\alpha < 0.4$) correlations (anticorrelations) are predicted between galaxies and background sources.

There are a number of observations of correlations between various types of QSOs and foreground galaxies. Here is a sampling of the recent literature. Radio selected 1 Jy QSOs at $z_s > 0.5$ (Kühr et al. 1981) are correlated with the APM Catalog galaxies, $z_l \sim 0.1 - 0.3$, (Seitz & Schneider 1995, Benítez & Martínez-González 1995, 1997, Norman & Williams 1999) on scales between a few arcminutes and a degree. Bright optically selected QSO from the LBQS Catalog (Hewett et al. 1995) are correlated with the APM galaxies on degree scales (Williams & Irwin 1998), while faint UVX selected QSO candidates are anti-correlated with galaxy groups on $\lesssim 10'$ scales (Croom & Shanks 1999). The amplitude of (anti)correlations varies between 30% and 1 – 2% depending on the angular scale and the details of each study.

As judged by their redshifts, QSOs and galaxies in all these studies are unconnected, therefore there are two possible physical reasons why these would appear to be associated in projection. One is weak lensing, as we have just described, the other is dust obscuration. However, a number of recent studies, if considered together, reject dust as the likely explanation.

Depending on the limiting magnitude of the QSO sample magnification bias will induce foreground galaxies to be either positively or negatively correlated with QSO. Bright end of the QSO number counts has a steep slope, $\alpha > 0.4$, and so $q > 1$; the opposite is true for QSO samples with faint limiting magnitudes, where $\alpha < 0.4$. And in fact q is observed to be > 1 in most of the above listed studies because most of them use bright QSOs. As one goes to fainter QSOs q seems to drop to ~ 1 , while faint QSOs, those in the Croom & Shanks study are anticorrelated with the intervening mass, i.e. $q < 1$. However to explain $q > 1$ and $q < 1$ cases with dust obscuration one needs to invoke two different types of dust: Galactic dust will obscure both QSOs and galaxies in some directions thus leading to positive correlations between the two populations, while dust intrinsic to lenses, i.e. galaxy clusters/groups will obscure QSOs in the direction of the lenses only, leading to anticorrelations. This double-type effect makes dust a rather contrived scenario.

Furthermore, if Galactic dust is responsible for the observed positive correlations one would expect the radio selected QSO samples to be less affected, and thus show smaller cross-correlation signal compared to optically selected QSOs. The observational situation is exactly opposite: 1 Jy QSOs are stronger correlated with APM galaxies (Norman & Williams 1999) than are LBQS QSOs (Williams & Irwin 1998) on similar angular scales.

Qualitative evidence not only rejects dust as the underlying physical cause, but also points to lensing. Amplitude and significance of correlations generally increase with brighter QSOs, as predicted by magnification bias. QSOs at intermediate redshifts, $z_s \sim 1 - 2$, i.e. those roughly at the optimal distance for being lensed by structures at $z_l \sim 0.1 - 0.3$ show the strongest correlations. Dust obscuration should show no preference for any particular QSO redshift range.

All evidence combined strongly suggests that lensing is responsible for the observations.

In fact, lensing would have been long accepted as the cause were it not for the unexpectedly large amplitude of the (anti)correlations. On small angular scales, $\lesssim 10'$ the non-linear growth of mass fluctuations with cosmic time produces the correct correlation strength; Dolag & Bartelmann (1997) and Sanz et al. (1997) reproduce the 1 Jy-APM correlations observed by Benítez & Martínez-González (1995, 1997). However, for correlations on larger scales, $\lesssim 1^\circ$, and anticorrelations on $\lesssim 10'$ scales (Croom & Shanks 1999) the strength of associations exceeds predictions by about a factor of 5-10.

There are three avenues within the lensing hypothesis for reconciling the model predicted and observed correlation amplitudes. One is to make the slope of the QSO number counts in the appropriate redshift range very steep. Williams & Irwin (1998) estimate the required slope α to be about 8. Because weak lensing induces small magnifications, the number counts slope of ‘lensed’ QSO, i.e. those seen in the directions of intervening mass concentrations should be almost as steep as the slope of the ‘unlensed’ QSOs. In other words, the overall QSO number counts slope should also be around 8. This is grossly inconsistent with the observed slope of $\sim 1.1 - 1.6$. We consider this option the least likely of the three.

The second alternative is to invoke mass density fluctuations on $\lesssim 2 - 10 h^{-1} \text{Mpc}$ scales ($10' - 1^\circ$ at $z_l \sim 0.1 - 0.3$) that are substantially larger than observations seem to indicate. Williams & Irwin (1998) and Croom & Shanks (1999) independently estimate that $\Omega\sigma_8$ should be about 3-4 to explain their respective results. The commonly accepted value for $\Omega^{0.6}\sigma_8$ is ≈ 0.6 , and is derived by two different methods: bulk flows in the nearby Universe and the abundance of rich galaxy clusters (Branchini et al. 1999, White et al. 1993). While scale-dependent biasing may allow one to increase the amplitude of mass fluctuations by 10 – 50%, an increase by a factor of 6-8 is outside the range of acceptable possibilities.

The third option is that the weak magnification regime of the lensing theory needs a revision. If future surveys support the results of present observations then this option will have to be considered seriously.

In principle many aspects of the currently accepted description of light propagation in an inhomogeneous medium can be questioned, for example the applicability of the Friedmann-Robertson-Walker metric and its weakly perturbed version in cosmological context, the validity of the general relativistic geodesic equation of motion as applied to light rays, etc. But the overwhelming success of the standard picture, which incorporates these concepts, in describing our Universe in general and observations of most types of gravitational lensing in particular suggests that the modifications to the standard description of lensing has to be sought within the existing framework. The standard lensing equation is the solution to the first order approximation of the full geodesic equation of motion for photons. There have been attempts in the literature to use the full geodesic equation to propagate light rays through a clumpy universe (Holz & Wald 1999, Tomita et al. 1999 and references therein), however these studies were focused on small angular scale lensing effects, and the equation was used in conjunction with a limited range of prescriptions

for mass fluctuations, and thus not fully explored.

Instead of taking on the full geodesic equation with all the higher order terms, our aim in this paper is to go one step beyond the standard lensing description, i.e. study the effect of the second order term(s) in the geodesic equation. The advantage of this approach is that we can derive useful analytic results, for example, an approximate form of the revised lensing equation (Section 3), and the equation for the increment in source magnification arising from retaining the second order term(s) (Section 4), and discuss qualitative predictions of the revised formulation (Section 5). With the help of numerical integrations we examine how the effects of the second order term(s) depend on the type of mass fluctuations populating the universe (Section 6 and 7).

2. Light propagation equation with second order terms included

The derivation of the standard lensing equation can be found in many places in the literature (Schneider et al 1992, and references therein; Dolag & Bartelmann 1997); here we follow the derivation presented by Kaiser (1998), but for simplicity adopt a spatially flat cosmological model. Unlike Kaiser and other authors we do not truncate the geodesic equation at the first order terms, but retain the second order term(s) as well.

The FRW spacetime metric with superimposed weak perturbations is given by

$$ds^2 = g_{\alpha\beta} dr^\alpha dr^\beta = a^2(\eta)[-(1 + 2\Phi)d\eta^2 + (1 - 2\Phi)(dx^2 + dy^2 + dz^2)], \quad (1)$$

where $a(\eta)$ is the scale factor, Φ is the Newtonian potential, η is the conformal time related to cosmic time, t though $dt = ad\eta$, and dx, dy, dz are the comoving separations between two adjacent points in space. Photon trajectories are solutions of the geodesic equation,

$$\frac{d^2 r^\alpha}{d\lambda^2} = -g^{\alpha\beta} \left(g_{\beta\nu,\mu} - \frac{1}{2} g_{\nu\mu,\beta} \right) \frac{dr^\nu}{d\lambda} \frac{dr^\mu}{d\lambda}, \quad (2)$$

where λ is the affine parameter, and $r^{0,1,2,3}$ stand for $\eta, x, y,$ and z (redshift is designated by z with a subscript, either z_l or z_s). The elements of the diagonal metric tensor $g_{\alpha\beta}$ can be read off from the line element, eq.(1). Let us write down the x -component of the geodesic equation keeping terms up to second order in small quantities, i.e. $\Phi, dx/d\lambda,$ and $dy/d\lambda$:

$$\frac{d^2 x}{d\lambda^2} \approx -\frac{\partial\Phi}{\partial x} \left(\frac{d\eta}{d\lambda} \right)^2 - \frac{\partial\Phi}{\partial x} \left(\frac{dz}{d\lambda} \right)^2 + 2 \frac{\partial\Phi}{\partial z} \left(\frac{dx}{d\lambda} \right) \left(\frac{dz}{d\lambda} \right). \quad (3)$$

The first two terms in this equation are the standard first order terms; the last term is the only surviving second order term. Changing the differentiation throughout to that with respect to z and using that $d\eta/dz = 1 - 2\Phi$ to first order, we get

$$\ddot{x} \approx -2 \frac{\partial\Phi}{\partial x} + 2 \frac{\partial\Phi}{\partial z} \dot{x}, \quad (4)$$

where the dots represent differentiation with respect to z , and x is the transverse comoving separation between a ray and the z -axis. A similar expression can be written for the y -component. This is the equation of motion for the x -component of a single light ray as it wanders through a spatially flat universe populated with small mass perturbations. The standard equation (see eq.[8] of Kaiser 1998) is eq.(4) minus the last term.

An alternative way to arrive at eq.(4) is by starting from Fermat's Principle which states that the path taken between two points in space, P_1 and P_2 , is a local extremum,

$$\delta \int_{P_1}^{P_2} d\eta = 0. \quad (5)$$

From the metric of eq.(1) and the condition that light rays are null geodesics we get

$$d\eta = (1 - 2\Phi)(dx^2 + dy^2 + dz^2)^{1/2}, \quad (6)$$

which can be rewritten as

$$n|\mathbf{t}| = 1, \quad (7)$$

where $n = (1 - 2\Phi)$ is the refractive index of the space-time described in eq.(1), $\mathbf{t} = \dot{x}\hat{\mathbf{x}} + \dot{y}\hat{\mathbf{y}} + \dot{z}\hat{\mathbf{z}}$ is the unit velocity vector of the light ray, and the dot represents $d/d\eta$. Equation (5) can now be rewritten as

$$\delta \int_{P_1}^{P_2} n|\mathbf{t}|d\eta = 0. \quad (8)$$

The integrand is an extremum when Euler-Lagrange equations are satisfied, so in the x -direction we must have

$$\frac{d}{d\eta} \left[\frac{\partial(n|\mathbf{t}|)}{\partial \dot{x}} \right] - \frac{\partial(n|\mathbf{t}|)}{\partial x} = 0, \quad (9)$$

which is simplified to a differential equation for light rays:

$$\frac{d}{d\eta} [n\mathbf{t}] - \nabla n = 0. \quad (10)$$

Rewriting this as

$$n\dot{\mathbf{t}} = \nabla n - \mathbf{t} \frac{d}{d\eta} n, \quad (11)$$

makes it apparent that we have arrived at the vector form of eq.(4). (This is the same as eq.[4.17] of Schneider et al. [1992], without the last term in their equation.) The term ∇n is the gradient of the refractive index evaluated in the coordinate system whose z -axis is aligned with the unperturbed light ray, while the term $\mathbf{t} dn/d\eta$ is along the direction of the actual ray. Thus the RHS of eq.(11) is the gradient of n in the plane perpendicular to the direction of the actual ray.

Because the last term in eq.(11) (i.e. the second order term) is small compared to the first one, is it neglected in the standard lensing equation. In physical terms this amounts to setting \dot{x} and \dot{y} to zero in eq.(11), so that \mathbf{t} is along the z -axis. In other words, this approximation, sometimes called the Born approximation, assumes that the actual ray is always parallel to the

unperturbed ray. In this paper we use the full eq.(11) and thus test the validity of the Born approximation.

Using (4) we now write down the comoving separation between two adjacent rays, say rays on the opposite sides of a small light bundle:

$$\Delta\ddot{x} \approx -2\Delta x \frac{\partial^2\Phi}{\partial x^2} - 2\Delta y \frac{\partial^2\Phi}{\partial x\partial y} + 2\frac{\partial\Phi}{\partial z}\Delta\dot{x}, \quad (12)$$

and similarly for the y -component. Here, the terms $2\Delta x \frac{\partial^2\Phi}{\partial z\partial x}\dot{x}$ and $2\Delta y \frac{\partial^2\Phi}{\partial z\partial y}\dot{x}$ are much smaller than the third term on the right hand side in the above expression, so they were omitted.

3. Approximate solution: revised lensing equation

Equation (4) without the second order term has an exact solution,

$$x = \theta_0 z - 2 \int_0^z \frac{\partial\Phi}{\partial x}(z - z') dz', \quad (13)$$

where θ_0 is the observed angle of the source with respect to the z -axis in the absence of perturbations. If all the mass fluctuations between the observer and the source are confined to a plane perpendicular to the z -axis then (13) reduces to the standard lensing equation. There is no useful solution for the full equation (4). To find an approximate solution in the weak lensing limit let us assume that \dot{x} is constant:

$$\dot{x} \approx x/z \approx \theta_0. \quad (14)$$

This is not a bad approximation in the weak lensing case where path deviations suffered by light rays are small. With this assumption the second order term in eq.(4) can be integrated by parts,

$$2\dot{x} \int_0^z dz' \left(\int_0^{z'} dz'' \frac{\partial\Phi}{\partial z''} \right) = 2\dot{x} \left(z \int_0^z \frac{\partial\Phi}{\partial z'} dz' - \int_0^z \frac{\partial\Phi}{\partial z'} z' dz' \right) = 2\dot{x} \int_0^z \frac{\partial\Phi}{\partial z'} (z - z') dz'. \quad (15)$$

Thus an approximate solution to equation (4) is

$$x \approx \theta_0 z - 2 \int_0^z \frac{\partial\Phi}{\partial x}(z - z') dz' + 2\dot{x} \int_0^z \frac{\partial\Phi}{\partial z'}(z - z') dz'. \quad (16)$$

This is the revised version of the ‘3-dimensional’ lensing equation (13). The equation for the transverse separation between two adjacent rays is then,

$$\Delta x \approx \Delta\theta_0 z \left[1 - 2 \int_0^z \left(\frac{\partial^2\Phi}{\partial x^2} + \frac{\partial^2\Phi}{\partial x\partial y} \right) \frac{z'(z - z')}{z} dz' + 2 \int_0^z \frac{\partial\Phi}{\partial z'} \frac{(z - z')}{z} dz' \right], \quad (17)$$

where we have approximated $\Delta\dot{x}$ by $\Delta\theta_0$, and set $\Delta x \approx \Delta y \approx \Delta\theta_0 z'$, similar to eq.(14), i.e. angular separation between two adjacent rays is constant to zeroth order.

4. Magnification of sources

If the source does not suffer much distortion and the x and y -axes are along the major and minor axes of the image, then the magnification of the image relative to the source is approximately

$$M \approx \left(\frac{z\Delta\theta_0}{\Delta x} \right) \left(\frac{z\Delta\theta_0}{\Delta y} \right). \quad (18)$$

The standard magnification in the weak lensing regime is then given by

$$M_{std} \approx 1 + 2 \int_0^z \left(\frac{\partial^2 \Phi}{\partial x^2} + \frac{\partial^2 \Phi}{\partial y^2} \right) z' \left(1 - \frac{z'}{z} \right) dz' \quad (19)$$

and the difference between M_{std} and magnification with the second order term is,

$$\Delta M = M_{2nd} - M_{std} \approx -4 \int_0^z \frac{\partial \Phi}{\partial z'} \left(1 - \frac{z'}{z} \right) dz'. \quad (20)$$

This additional magnification depends on the gradient of the Newtonian potential along the z -axis, or along the line of sight to the source. Equation (20) was found to be in excellent agreement with the results of numerical integrations (see below) for magnifications $M_{std} \lesssim 1.3$. This range is more than sufficient for the present study; magnifications typically produced by smoothed large scale structures on $\lesssim 1^\circ$ scales are less than 1%. For example, mass fluctuations associated with the $18.5 \leq m_R \leq 20.0$ APM galaxies in Williams & Irwin study are of the order 1.005.

5. Properties of the equation

Qualitative consequences of the second order term in the geodesic equation can be assessed from eq.(17) and (20). Let us consider a single positive mass fluctuation between us and the source. $\partial\Phi/\partial z$ will be negative between us and the lens, and because of the $(1 - z'/z)$ weighting in the last term of eq.(17) it will decrease Δx , i.e. increase magnification. The opposite is true for fluctuations of negative $\delta\rho/\rho$. Alternatively, looking at eq.(11) we see that the second order term increases the bending of the rays around positive and negative potential wells beyond what is predicted by the standard first order term. Thus the second order term reinforces the amplitude of (de)magnification predicted by the standard formulation.

According to eq.(17) both Δx and Δy -components of the beam's cross section are affected in the same way by the second order term, i.e. a factor proportional to $\int_0^z \frac{\partial \Phi}{\partial z'} \left(1 - \frac{z'}{z} \right) dz'$ is added to both, therefore magnification along the x -direction is not at the expense of magnification in the y direction, and so for small magnifications there will be no change in the lensing-induced shape distortion of the image. This was verified by the numerical integrations of eq.(12).

When a significant lens is encountered, meaning the projected mass density fluctuation is high, the middle term in eq.(17) becomes large, as it is related to the mass density through the Poisson equation. Thus the magnification is dominated by the second derivatives of Φ , and the

extra magnification supplied by the second order term, ΔM is negligible compared to $(M_{std} - 1)$. In other words the standard equation is completely adequate in the regions of high density, for example in galaxy clusters and near individual galaxies.

An important aspect of the standard lensing equation is that not all equal amplitude mass fluctuations between the observer and the source contribute equally to the source magnification; eq.(19) shows that the fluctuations are weighted by $z'(1 - z'/z)$, i.e. lenses approximately half way between the source and the observer are most influential. $\partial\Phi/\partial z$ in eq.(17) and (20) is weighted by $(1 - z'/z)$, thus the lenses closer to the observer contribute more through ΔM . In practice it is probably the combination of the amplitude of fluctuations, their physical scale and proximity to the observer that determines their relative contributions to ΔM . For example, because $(1 - z'/z)$ depends on the distance only weakly high frequency fluctuations will mutually cancel out, and will not contribute significantly to ΔM . ΔM is probably dominated by the ‘last screen’ of large scale structure, like superclusters, voids and filaments, located closer to the observer than the standard optimal lensing distance.

This is an interesting point in the light of some of the observational results. A few cross-correlation studies seem to indicate that the galaxies most strongly correlated with the QSOs are not the ones at the optimal lensing redshifts but are somewhat closer than that to the observer. This was stressed by Bartelmann & Schneider (1993) who reanalyzed Fugmann (1990) result of correlations between Lick Catalog galaxies and 1 Jy sources. It was also found to be the case by Williams & Irwin (1998) who show that correlations are strongest for $z_{QSO} \geq 1$. The optimal lens location in the Einstein-de Sitter universe model for sources at $z_{QSO} \geq 1$ would be 0.4, while the galaxies in their study lie at $z_l \sim 0.2$.

Equation (20) for ΔM shows that flux is conserved with the addition of the second order term, as $\partial\Phi/\partial z$ will average out to zero for a collection of sources.

Finally, because the second order term depends on $\partial\Phi/\partial z$ it is essential that the continuous, 3-dimensional nature of the mass fluctuations is taken into account. If the effect of the second order term proves to be non-negligible then the treatment of weak QSO lensing based on multiple-plane formalism, where the standard lensing equation is solved successively on many 2D planes stacked perpendicular to the optical axis, should not be used.

We will return to some of the qualitative remarks made in this Section in Section 7, where we discuss the results of numerical integrations of eq.(12).

6. Application of the equation

6.1. Numerical integrations

To study the effect of the second order term further we need to consider an inhomogeneous mass distribution in the Universe, solve eq.(12) for many lines of sight and compute relevant output quantities, like distribution of magnifications, average magnification, etc. Given the simplicity of the approximate solution, eq.(17), this can be done analytically for simple mass distributions. For an arbitrary mass distribution a numerical integration approach is preferred. We use 5th order Runge-Kutta method to integrate eq.(12) and its y -component counterpart. In principle, as a light bundle propagates through a clumpy medium the path of its central ray will deviate from the fiducial ray in the absence of perturbations; however, one can ignore this effect in the weak lensing regime and evaluate the gradients of the Newtonian potential in eq.(12) along the fiducial central ray. When integrating eq.(12) we use boundary conditions at the observer; for every line of sight we start with two images seen by the observer, each one confined to the x - and y -axis entirely, and propagate these backwards to the redshift of the source. The shape, size and orientation of the two final sources per line of sight allows us to solve for the four components of the total magnification matrix. All sources are located at $z_s = 1.5$, typical redshift of QSOs in correlation studies.

6.2. Mass density fluctuations

We are primarily interested in how the weak lensing model predictions are affected by the inclusion of the second order term, in particular if the differences in the standard vs. revised predictions depend on the type of mass density fluctuations present in the universe. Therefore we pick two rather different, but simple mass fluctuation scenarios: randomly distributed spherically symmetric mass clumps, and a Gaussian random-phase field.

In both the scenarios we limit ourselves to large scale structures only, and do not attempt to include the lensing effects of smaller, more compact objects like individual galaxies and galaxy clusters. The computed correlation amplitude will not be affected by this exclusion: Theoretical calculations of weak lensing induced correlations effectively smooth out density fluctuations on scales below the correlation scale. This is seen clearly from equation (13) of Dolag & Bartelmann (1997), where the cutoff is imposed by the filter function $F(k, \phi)$.

On large scales the linear growth of mass density fluctuations is an adequate assumption; therefore at every cosmic epoch we scale the amplitude of fluctuations by $a(t) = 1 + z_t$.

6.2.1. Model #1: Clumps

This model for the mass distribution is motivated by the observation that the large scale structure looks like a network of walls, voids and filaments, i.e. coherent structures spanning tens

of Megaparsecs. Therefore we represent the mass fluctuations by a collection of many spherically symmetric clumps. We have experimented with a number of different density profiles, including non-singular isothermal sphere, top hat, and Hernquist profile, $\rho \propto [r(1 + r/r_0)^3]^{-1}$. Qualitatively the results described below are similar for all types of mass clump profiles provided the physical scale of the clumps is about the same. In what follows we use clumps described by a Newtonian potential, $\Phi(r) \propto -e^{-r/r_c}$, where r is comoving distance from the clump center, and r_c is its scale length. This particular shape was chosen because the potential falls off quickly so that the influence of the mass clumps does not extend over scales comparable to the Hubble length. The mass profile of a clump is

$$\rho(r) \propto \frac{e^{-r/r_c}}{rr_c} \left(2 - \frac{r}{r_c}\right). \quad (21)$$

The profile has a central mass peak ($r < 2r_c$) and is surrounded by a shallow region of the opposite density. The clumps are quite compact: for $r_c = 0.1 \frac{c}{H_0}$ the density drops by a factor of ~ 50 between $r_c/10$ and r_c , and by a factor of ~ 20 between r_c and $3r_c$. The mass enclosed within r of each clump goes as $e^{-r/r_c} r^2 r_c^{-1}$, and asymptotically approaches zero. We use clumps of positive and negative central mass density, so even in a small volume the statistical expectation value for the net excess mass density is zero. This is in accord with the equations derived in Sections 2, 3 and 4 which assume a flat space geometry.

The clumps are randomly distributed in space with a typical interclump separation of about $70h^{-1}\text{Mpc}$. The line of sight from the observer to the source is completely immersed in a sea of clumps. All clumps are identical, with $r_c = 0.1 \frac{c}{H_0} = 300h^{-1}\text{Mpc}$ which is larger than the interclump separation. Because of this the typical radius of the net structures formed by the superposition of clumps is about $0.05 \frac{c}{H_0} = 150h^{-1}\text{Mpc}$, comparable to the size of the largest superclusters seen in the nearby Universe (Batuski et al. 1999). The rms fluctuations of mass in spheres of $R = 300h^{-1}\text{Mpc}$ is 0.012, comparable to, or somewhat higher than the standard $\sigma_8 = 1$ normalized CDM value. The amplitude of fluctuations in this model grows slowly with decreasing scale; the fractional contribution to σ_8 is small. We will return to the discussion of the amplitude of mass fluctuations later, in Section 7. In the redshift range $z_l = 0.1 - 0.3$, the location of the galaxies used in the cross-correlation studies, the average projected separation between two adjacent clumps is $25h^{-1}\text{Mpc}$, or about 2.5° , comparable to the angular scale of observed QSO-galaxy cross-correlations.

6.2.2. Model #2: Gaussian random field

Here we assume that the fluctuations are represented by a Gaussian random field. The form of the power spectrum was taken from Peacock (1997). To make a fair comparison with the clumps model we limit the power spectrum to a range of wavenumbers between $k_{low} = 2\pi(2r_c)^{-1} = 0.01h\text{Mpc}^{-1}$ and $k_{high} = 2\pi(0.5r_c)^{-1} = 0.04h\text{Mpc}^{-1}$. In this region the shape of the power spectrum is $P(k) \propto k$. The phases of the various modes are uncorrelated.

7. Results of numerical integrations

7.1. General considerations

For every line of sight numerical integration of eq.(12) yields source magnification. Since we are interested in the cross-correlation between sources and the lensing mass, we first need to relate the source magnifications to the cross-correlation function.

Williams and Irwin (1998) derived a relation, applicable in the weak lensing regime, between QSO-galaxy correlation function, $\omega_{QG}(\theta)$, and the autocorrelation function of the foreground galaxies used in the analysis, $\omega_{GG}(\theta)$ (their eq.[6]): $\omega_{QG}(\theta) \approx (2\tau/b)(2.5\alpha - 1)\omega_{GG}(\theta)$, where τ is the total optical depth of the lensing slab of matter traced by the APM galaxies, and b is the bias parameter. The factor $(2\tau/b)$ is the proportionality coefficient between $(M - 1)$, ‘magnification excess’ of a source, and normalized galaxy number excess, $(\sigma - 1)$, both M and σ referring to the same patch of the sky. In the weak lensing regime $(M - 1)$ and $(\sigma - 1)$ are linearly related in both the standard and revised lensing formulations, but the coefficient is different. Thus for either formulation we can write

$$\omega_{QG}(\theta) \approx \langle (M - 1)/(\sigma - 1) \rangle (2.5\alpha - 1)\omega_{GG}(\theta), \quad (22)$$

where the brackets indicate the typical value over many lines of sight. Without evaluating $\omega_{QG}(\theta)$ itself, eq.(22) allows us to derive an expression for the change in the predicted correlation function resulting from adding the second order term to eq.(4), while keeping the galaxy distribution, $p(\sigma|\theta)$ and the slope of source number counts, α the same:

$$\frac{\omega_{QG,2nd}(\theta)}{\omega_{QG,std}(\theta)} = \left\langle \frac{(M_{2nd} - 1)}{(M_{std} - 1)} \right\rangle. \quad (23)$$

The quantity $(M_{2nd} - 1)/(M_{std} - 1)$ for any line of sight has an interesting property of being independent of the *amplitude* of mass density fluctuations, while being sensitive to the *shape* of the fluctuations. This is readily seen from eq.(19) and (20): both versions of $(M - 1)$ are proportional to Φ . Therefore the change in ω_{QG} is the same regardless of the actual amplitude of fluctuations or the magnifications induced by the mass structures, so long as their shape remains the same.

Although the actual values of magnifications are not important, the values presented below are comparable to what one expects from the smoothed large scale structure, i.e. $\lesssim 1\%$.

All the integrations described below conserve flux. Flux is considered to be conserved if the ratio of the total amount of flux received by all observers distributed in a spherical shell around a source to the total flux emitted by that source is 1. For any given observer that ratio is just $1/M$; the average $1/M$ over a 1000 or so observers in each set of integrations was found to be less than one standard deviation of the mean away from unity.

We now describe the results for each of the two mass fluctuation models.

7.2. Mass density fluctuations

7.2.1. Model #1: Clumps

Each point in the top panel of Figure 1 represents the magnification of a source computed using the standard and second order formulations: M_{std} and M_{2nd} , respectively. It is apparent that including the second order term has a small but non-negligible effect on the computed magnifications. The bottom panel, which shows the residuals $\Delta M = M_{2nd} - M_{std}$ vs. M_{std} , demonstrates that M_{2nd} is, on the average, more extreme than M_{std} , in other words, the second order term increases the computed magnification of the source if $M_{std} > 1$, and decreases it if $M_{std} < 1$. This effect was already noted in Section 5. The fractional change is not very large; on the average $\Delta M / (M_{std} - 1) \approx 0.2$.

Do these results alter the predicted amplitude of QSO-galaxy correlation function? Figure 2 shows $(M_{2nd} - 1) / (M_{std} - 1)$ as a function of the projected angular distance between the source and the nearest mass clump of either positive or negative central density. The only clumps considered here are in the redshift range $0.1 - 0.3$, to simulate the observed situation. The angular scale of correlations includes the observational scale of $\lesssim 1^\circ$. The median of all the $(M_{2nd} - 1) / (M_{std} - 1)$ points is 1.1, i.e. the amplitude of the cross-correlation function is increased by 10% compared to the standard lensing equation. As the reader will remember from the Introduction, an increase by a factor of $\gtrsim 5$ is needed to reconcile observations with theory.

The solid points in the plot represent sources (lines of sight) with $M_{2nd} > 1.001$, an arbitrary cutoff designed to separate out about half the magnification values. The median of the solid points is very similar to the one quoted above, i.e. 1.1, but the dispersion in the points is much smaller, and so it is more obvious that the points prefer to lie above the $(M_{2nd} - 1) / (M_{std} - 1) = 1$ line. In a simple case where the source number counts truncate at a flux just below our detection limit the solid points will represent a flux limited sample of observed sources.

Note that about half of all the points in this plot represent $M_{std} < 1$, i.e. demagnifications. In such cases ΔM values tend to be less than zero, therefore $(M_{2nd} - 1) / (M_{std} - 1) > 1$, and lensing induced anti-correlations are also enhanced by the second order term.

As was pointed out in Section 5 with the help of eq.(20), the presence of the second order term in eq.(4) may change the redshift of the optimal lenses compared to the standard formulation; it may ‘move’ the most effective lenses, for fixed source redshift, closer to the observer. The numerical integrations indicate such an effect. We have divided the nearby universe into four slices oriented perpendicular to the line of sight to the sources. The slices are: $z_l = 0.05 \rightarrow 0.1$, $0.1 \rightarrow 0.2$, $0.2 \rightarrow 0.3$, and $0.3 \rightarrow 0.4$. In each slice we compute the median value of $(M_{2nd} - 1) / (M_{std} - 1)$ for sources found within angle θ of at least one clump. Only clumps of positive central density were used in this exercise to emulate the observations where QSOs are (anti)correlated with regions of galaxy excess. The results are plotted in Figure 3. Angle θ was set to 0.5° (solid), 0.75° (dotted), and 1° (dashed), comparable to the angular scale of observed correlations. Mass concentrations

in all redshift slices are more correlated with the background sources than the standard lensing formalism would predict, however, the increase in the correlation amplitude is larger for $z_l \leq 0.2$ slices than for the $z_l \geq 0.2$ slices, i.e. the inclusion of the second order term moves the redshift of the optimal (most correlated) mass fluctuations closer to the observer.

How do the results change if we adopt a different value for the clump length scale, r_c ? The effect of the second order term, evaluated with $(M_{2nd} - 1)/(M_{std} - 1)$ declines rapidly as r_c is reduced by a factor of 3 or larger. This is easy to understand; the effects of small scale density fluctuations on the net $\partial\Phi/\partial z$ cancel out as eq.(20) is integrated between the source and the observer. Only the effects of larger scale fluctuations, however small in amplitude, will remain.

7.2.2. Model #2: Gaussian random field

Figure 4 compares M_{std} with M_{2nd} for the Gaussian random field mass fluctuation prescription, and is equivalent to Figure 1 of the clumps model. Though Gaussian random field does respond to the second order term, the change in magnification is very much smaller than in the clumps scenario, therefore there will be virtually no increase, over the standard lensing formulation, in the predicted amplitude of cross-correlations if a Gaussian random-phase field describes the mass density fluctuations on large length scales.

Why does the inclusion of the second order term make a difference in the weak lensing model predictions when a clumps density model is used, while no effect is seen when the density field is Gaussian? As we have already mentioned the normalization of the power spectrum has no effect on $(\omega_{QG,2nd}/\omega_{QG,std})$. If normalization is increased the magnification labels on both the axis of Figure 4a will change, but the slope of the line defined by the points will not. Same is true for Figure 1a of the clumps model. The physical scale of density fluctuations is the same in both the models, so that too can be ruled out as the source of the difference in the results. The exact form of the clumps is also not a factor; we have tried a number of profile shapes, and all yielded very similar results. We are led to conclude that the difference is due to the shape of the density fluctuations in the clumps vs. Gaussian random field models, in particular it is due to the large scale coherent, i.e. non-Gaussian nature of the clumps.

One can arrive at the same conclusion by considering the physical content of eqs.(11) and (4). According to eq.(4) the second order term introduces some extra bending of the light rays towards positive mass inhomogeneities and away from negative ones. In a density field dominated by small-scale incoherent structures, like our Gaussian random field, the rays are bent many times in opposing directions as they travel from the source to the observer, thereby averaging to a straight line, a situation well described by the standard lensing approach.

8. Summary and Conclusions

We have extended the standard lensing formulation to include the next order term (second order term in the geodesic equation) in the hope that it will make a significant difference in the predicted amplitude of weak lensing induced QSO-galaxy correlations, which is currently at least a factor of 5 smaller than observed. Depending on the type of the mass density fluctuations populating our model universe, we can obtain up to a $\sim 10\%$ increase in the amplitude of the correlations, i.e. not enough to reconcile theory with existing observations.

Even though the increase is small, qualitative aspects of the updated weak lensing formulation bring us closer to the properties of the observed correlations. The revised source magnifications correlate with, but are more extreme than the magnifications computed using the standard formulation, i.e. typically $(M_{2nd} - 1)/(M_{std} - 1)$ is greater than 1, which increases the amplitude of predicted lensing-induced correlations. Furthermore, the redshift of the optimal lenses for cross-correlations with sources at a given redshift is closer to the observer than what the standard formulation would predict. This is consistent with observational results. It is important to note that the second order term affects only the predictions of the lensing theory which deal with weak statistical lensing of point sources. As we have shown using eq.(17) and (20) and numerical integrations, image elongation, i.e. weak shear lensing, and strong lensing theory are not altered.

Potentially the most important result of the present work is that not all types of cosmic density fluctuations are sensitive to the presence of the next higher order term in the lensing equation. Only large-scale, coherent, i.e. non-Gaussian structures show an increase in ω_{QG} with the revised formulation. This can be intuitively understood in terms of eq.(11) and (4) (see end of previous Section), and quantified with eq.(20), which states that the increase in magnification induced by the second order term is proportional to a weighted integral of $d\Phi/dz$ over the line of sight. The integral will tend to be smaller when the phases of the modes comprising the density and the potential field are uncorrelated, compared to a density fluctuation model dominated by coherent structures. Note that the increase in the predicted cross-correlation, $(\omega_{QG,2nd}/\omega_{QG,std})$ does not depend on the amplitude of the mass fluctuations, only on their form.

The work presented here is preliminary, however, if the avenue we have taken proves to be correct, i.e. if second order, and possibly higher order terms in the geodesic equation of motion of photons are important for weak lensing induced QSO-galaxy correlations, then these correlations will give us the means to study the type of mass structures present on the largest scales, in particular to test the Gaussianity of the large scale fluctuations and thus shed light on the physical processes in the early Universe that gave rise to the present day structures.

I am deeply indebted to Prasenjit Saha for numerous invaluable conversations on the subject and many helpful suggestions. I am grateful to the anonymous referee for further elucidating the physical meaning of the second order term.

REFERENCES

- Bartelmann, M., & Schneider, P. 1993, *A & A*, 268, 1
- Batuski, D. J., Miller, C. J., Slingsend, K. A., Balkowski, C. Maurogordato, S., Cayatte, V., Felenbok, P., & Olowin, R. 1999, *ApJ*, 520, 491
- Benítez, N., & Martínez-González, E. 1995, *ApJ*, 448, L89
- Benítez, N., & Martínez-González, E. 1997, *ApJ*, 477, 27
- Croom, S. M., & Shanks, T. 1999, *MNRAS*, submitted, astro-ph/9905249
- Branchini, E. et al. 1999, *MNRAS*, accepted, astro-ph/9905249
- Dolag, K., & Bartelmann, M. 1997, *MNRAS*, 291, 446
- Fugmann, W. 1990, *A & A*, 240, 11
- Hewett, P. C., Foltz C. B., & Chaffee, F. H. 1995, *AJ*, 109, 1489
- Holz, D. E. & Wald, R. M. 1997, astro-ph/9708036
- Kaiser, N. 1998, *ApJ*, 498, 26
- Kühr, H., Witzel, A., Pauliny-Toth, I., & Nauber, U. 1981, *A & ASS*, 45, 367
- Peacock, J. A. 1997, *MNRAS*, 284, 885
- Norman, D. & Williams, L. L. R. 1999, *AJ*, submitted, astro-ph/9908177
- Sanz, J., Martínez-González, E., & Benítez, N. 1997, *MNRAS*, 291, 418
- Schneider, P., Ehlers, J., & Falco, E. 1992, *Gravitational Lenses* (Berlin: Springer-Verlag)
- Seitz, S., & Scheider, P. 1995, *A & A*, 302, 9
- Tomita, K., Premadi, P., & Nakamura, T. T. 1999, *Prog. Theor. Phys. Suppl.* 133, 85
- White, S. D. M., Efstathiou, G. Frenk, C. S. 1993, *MNRAS*, 262, 1023
- Williams, L.L.R., & Irwin, M. 1998, *MNRAS*, 298, 378

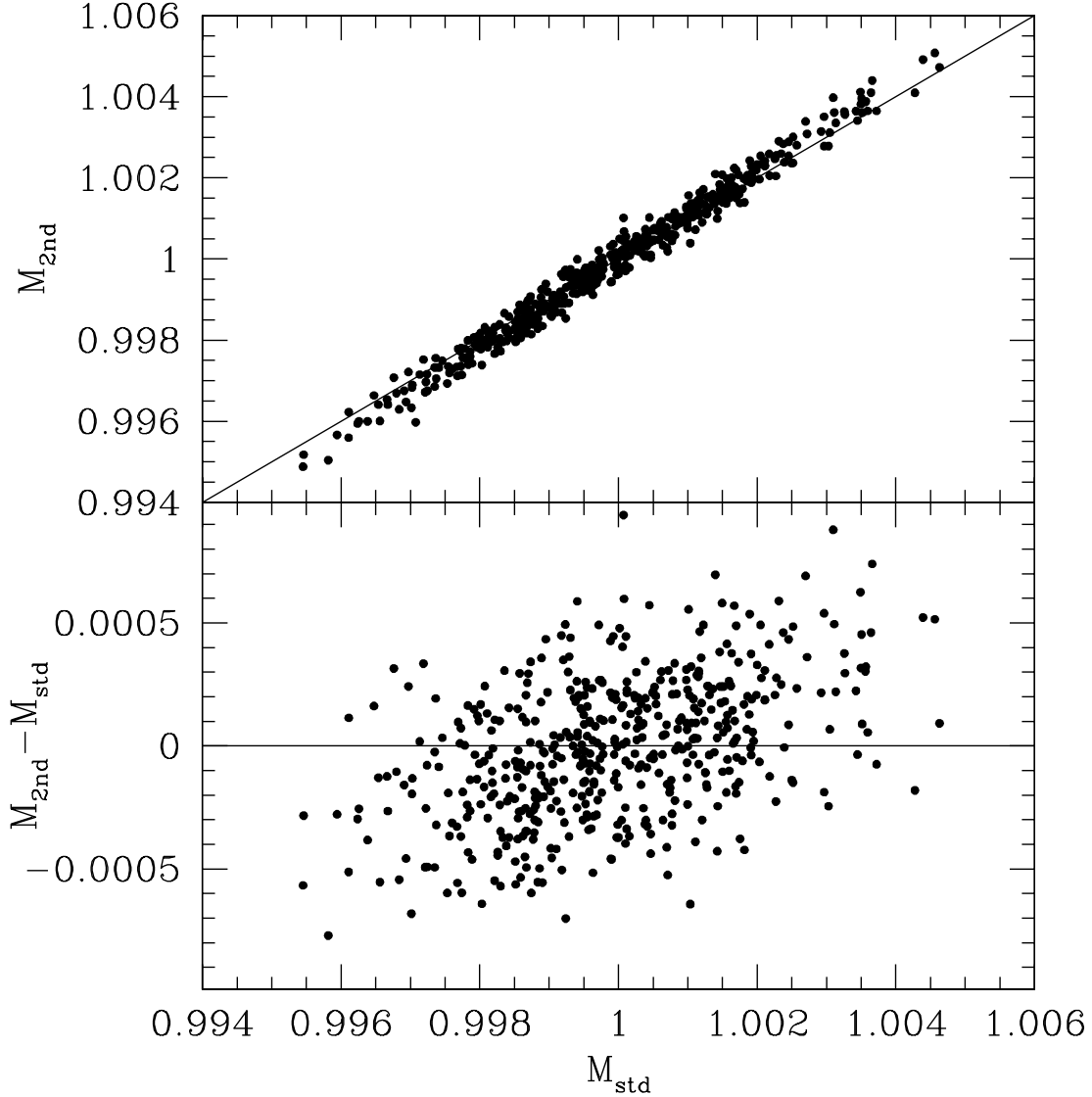


Fig. 1.— Magnification of sources obtained using the standard lensing formalism, M_{std} , and magnification computed when the second order term in the geodesic equation is included, M_{2nd} . The mass fluctuations in this model universe are build up with a collection of randomly distributed spherical clumps of positive and negative central density. See Section 6 for details. The residuals, ΔM , plotted in the bottom panel, are positively correlated with M_{std} , i.e. inclusion of the second order term enhances (de)magnifications.

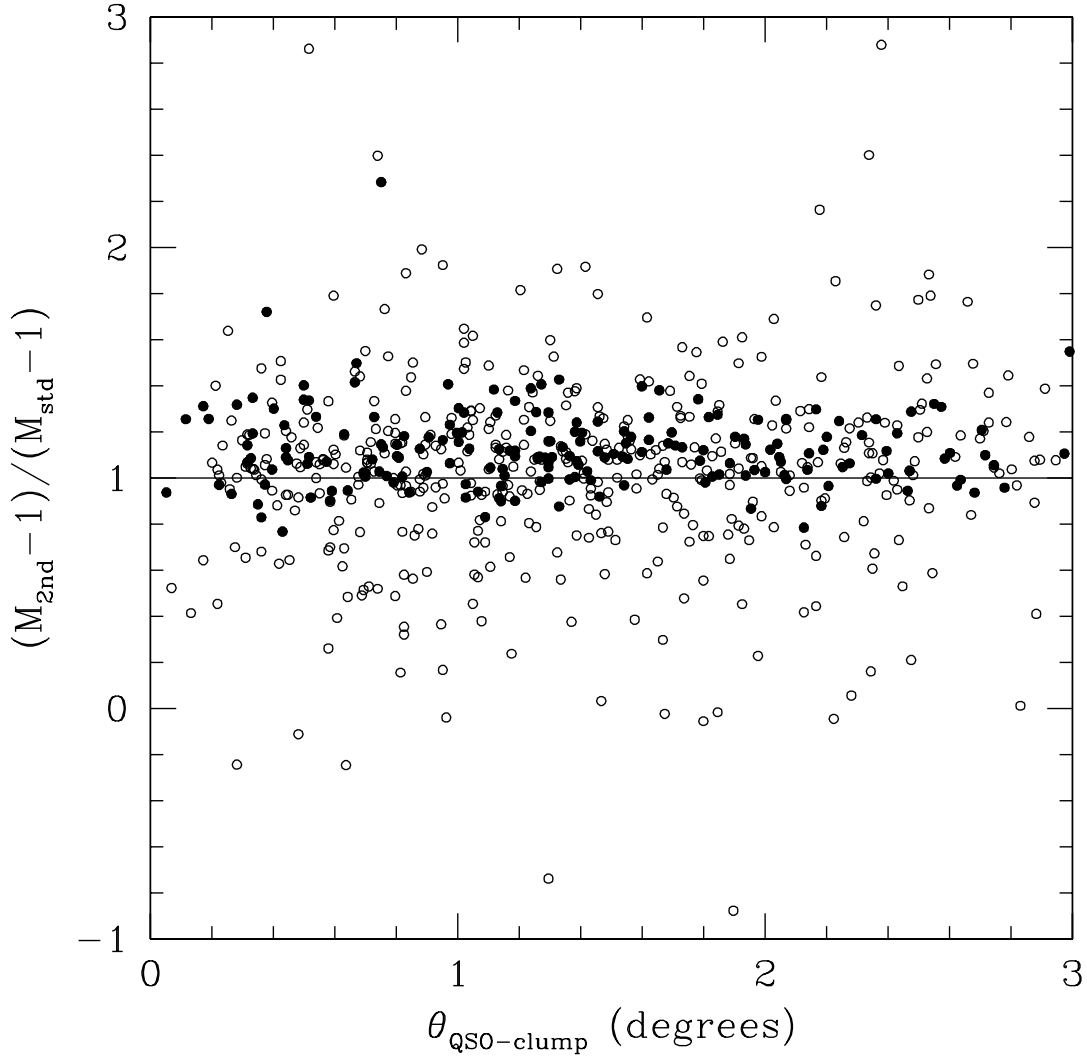


Fig. 2.— The factor by which cross-correlations are increased is plotted against the projected distance to the nearest mass clump in the $z_l = 0.1 - 0.3$ redshift range. All the sources are at $z_s = 1.5$, and mass density fluctuations are represented by a collection of spherically symmetric mass clumps (see Section 6 for more details.) The median increase in the amplitude of ω_{QG} is 1.1. The solid points are those with $M_{2\text{nd}} > 1.001$ and have the same median. Correlations are increased on all angular scales.

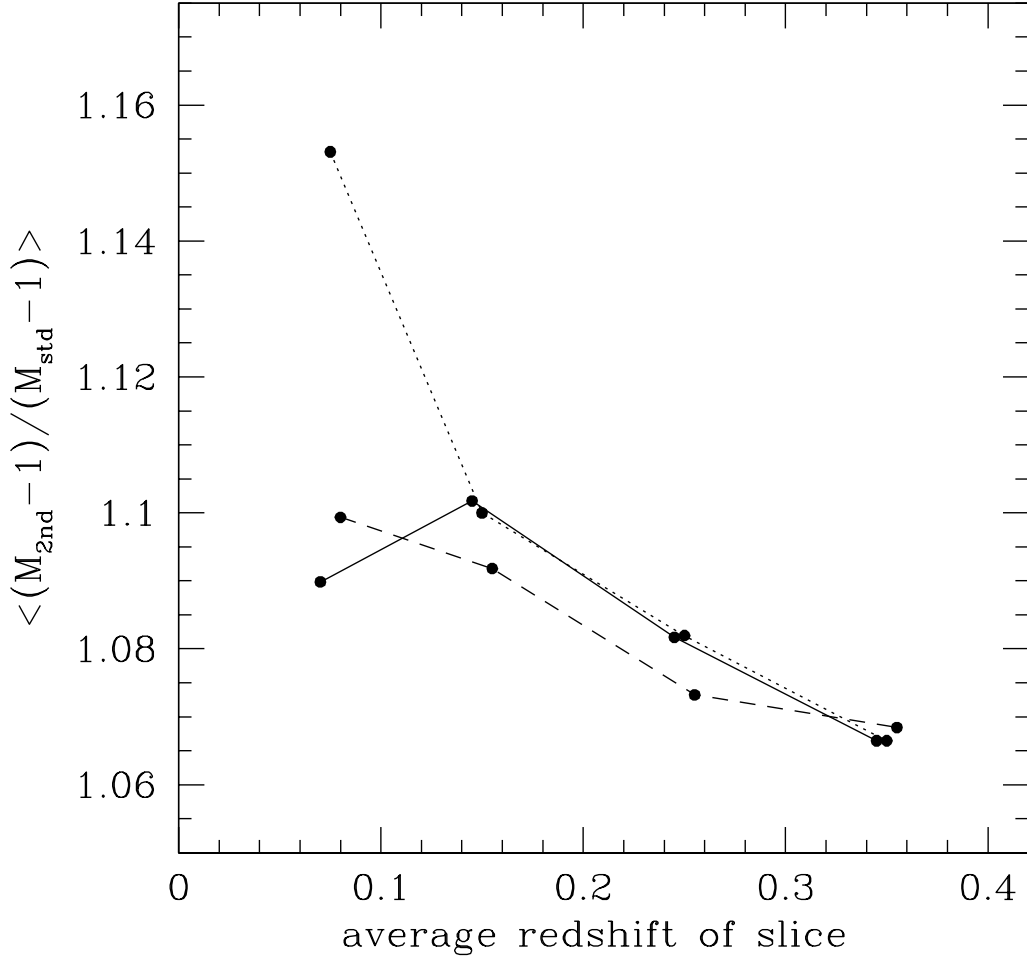


Fig. 3.— Change in the amplitude of predicted cross-correlation function between $z_s = 1.5$ sources and mass distribution in four low-redshift slices, $z_l = 0.05 \rightarrow 0.1$, $0.1 \rightarrow 0.2$, $0.2 \rightarrow 0.3$, and $0.3 \rightarrow 0.4$. In each of the four redshift slices the median value of $\langle (M_{2nd} - 1) / (M_{std} - 1) \rangle$, equal to $(\omega_{QG,2nd} / \omega_{QG,std})$, was computed for sources lying within θ of a mass clump (positive central mass density clumps were used here). Angle θ was chosen to be comparable to the angular scale of observations, $\theta = 0.5^\circ$ (solid), 0.75° (dotted), and 1.0° (dashed). (Note that the number of lines of sight contributing to the twelve points of the plot varies significantly: the $\theta = 0.5^\circ$, $z_l = 0.05 \rightarrow 0.1$ point has 20 lines of sight, while $\theta = 1.0^\circ$, $0.3 \rightarrow 0.4$ point has ~ 1700 .) The inclusion of the second order term in the geodesic equation preferentially increases the amplitude of correlations for more nearby lenses, thus ‘moving’ the optimal lenses closer to the observer, compared to the standard optimal lensing distance.

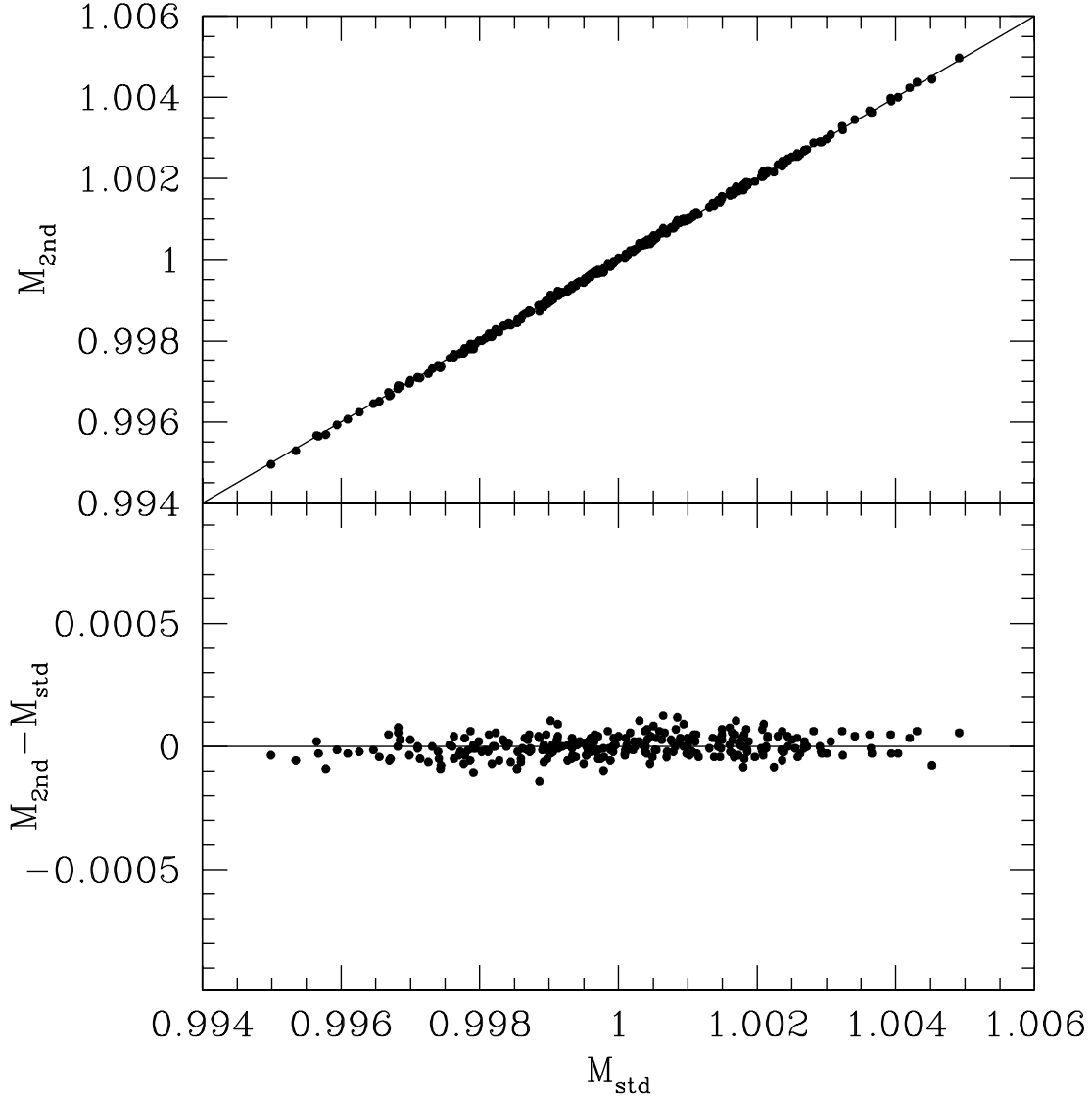


Fig. 4.— Similar to Figure 1, except the mass fluctuations here are described by a Gaussian random-phase field, with the power spectrum, $P(k) \propto k$, and limited to the range of wavenumbers between $k_{\text{low}} = 2\pi(2r_c)^{-1} = 0.01h\text{Mpc}^{-1}$ and $k_{\text{high}} = 2\pi(0.5r_c)^{-1} = 0.04h\text{Mpc}^{-1}$. The residuals, ΔM are much smaller than in Figure 1.